Biochemical Pharmacology 80 (2010) 179–187

Contents lists available at ScienceDirect

Biochemical Pharmacology

journal homepage: www.elsevier.com/locate/biochempharm

Functional characterization of gefitinib uptake in non-small cell lung cancer cell lines

Maricla Galetti [a,1], Roberta R. Alfieri [a,1,*], Andrea Cavazzoni [a], Silvia La Monica [a], Mara Bonelli [a], Claudia Fumarola [a], Paola Mozzoni [b,c], Giuseppe De Palma [d], Roberta Andreoli [b,c], Antonio Mutti [b], Marco Mor [e], Marcello Tiseo [f], Andrea Ardizzoni [f], Pier Giorgio Petronini [a]

[a] Department of Experimental Medicine, University of Parma, Via Volturno 39, 43100 Parma, Italy
[b] Department of Clinical Medicine, Nephrology and Health Science, Laboratory of Industrial Toxicology, University Hospital of Parma, Italy
[c] National Institute of Occupational Safety and Prevention (ISPESL), Research Center at the University of Parma, Italy
[d] Department of Experimental and Applied Medicine, Section of Occupational Medicine and Industrial Hygiene, University of Brescia, Italy
[e] Pharmaceutical Department, University of Parma, Parma, Italy
[f] Division of Medical Oncology, University Hospital of Parma, Italy

ARTICLE INFO

Article history:
Received 1 February 2010
Accepted 26 March 2010

Keywords:
Lung cancer
EGFR
Gefitinib
Uptake

ABSTRACT

Gefitinib, an inhibitor of epidermal growth factor receptor tyrosine kinase, has been developed and approved for treatment of advanced non-small cell lung cancer (NSCLC).

In this study, we investigated the uptake of gefitinib in gefitinib-sensitive and -resistant NSCLC cell lines. The transport system was temperature-dependent, indicative of an active process and sodium- and potential-independent. Moreover, high cell densities and low extracellular pH significantly reduced the uptake of gefitinib. Inhibitors of the human organic cation transporter 1 (hOCT1) significantly decreased gefitinib uptake; however, gefitinib was not a substrate for hOCT1 or hOCT2 in overexpressing HEK293 cells. Interestingly, gefitinib significantly reduced uptake of the hOCT prototypical substrate MPP suggesting that gefitinib may exert an inhibitory effect on the intracellular accumulation of drugs transported by hOCT1 and hOCT2.

After 15 min of treatment at 1 μM (the maximum plasma concentration of gefitinib obtained at the clinically relevant dose) gefitinib accumulated within the cell in resistant-cell lines at concentrations similar or even higher than in gefitinib-sensitive cells tending to rule out an alteration in drug uptake as a mechanism of resistance to gefitinib treatment.

Moreover, our results suggest that the extrusion of lactate by crowded cells may contribute in decreasing the pH, which in turn can influence the uptake of gefinitib and as a result the inhibition of EGFR autophosphorylation.

1. Introduction

The epidermal growth factor receptor (EGFR) is a major target of molecular anticancer therapy. Two main strategies targeting EGFR have been developed: monoclonal antibodies, directed against the extracellular domain of EGFR, that inhibit its phosphorylation/activation and stimulate internalization and small-molecule inhibitors of the tyrosine kinase domain (tyrosine kinase inhibitors, TKIs) [1]. Gefitinib is an orally active, selective EGFR TKI used in the treatment of patients with advanced NCSLC [1,2]. This drug produces tumor regression in 10–20% of patients with heavily pretreated NSCLC [2]. Nevertheless, it appears that greater benefit can be obtained with EGFR TKIs in some patient subgroups, such as females, never smokers, Asians and patients with adenocarcinoma histology. Although clinical characteristics may identify candidates for EGFR TKIs, patient selection should rely on the biological features of the tumor, in particular the presence of EGFR gene mutations.

However, not all the tumors having activating mutations are associated with an enhanced response mainly because of additional genetic lesions that relieve the tumor of its dependence on the EGFR signaling pathways [3]. Moreover, acquired resistance occurs in virtually all NSCLC tumors that initially respond to EGFR TKIs therapy. In approximately half of NSCLC cases that showed an initial response to reversible EGFR tyrosine kinase inhibitors and subsequently progressed, resistance was associated with the emergence of a secondary mutation within the EGFR kinase domain: substitution of threonine 790 with methionine (T790 M). Additional mechanisms of resistance have been described, such as

* Corresponding author. Tel.: +39 521 033766; fax: +39 521 033742.
E-mail address: roberta.alfieri@unipr.it (R.R. Alfieri).
[1] These authors contributed in equal part to this study.

0006-2952/$ – see front matter © 2010 Elsevier Inc. All rights reserved.
doi:10.1016/j.bcp.2010.03.033

the activation of alternative tyrosine kinase receptors (IGF-1R), amplification of the MET gene and constitutive activation of signaling pathways downstream of EGFR [4–7]. Resistance can also be mediated by a reduced intracellular level of drug resulted from poor uptake, increased metabolism or enhanced efflux. Membrane transporters have been found to play an important role in the distribution and accumulation of anticancer drugs and in chemosensitivity/chemoresistance [8].

Although gefitinib is a known inhibitor of the efflux transporter ABCG2 (ABC subfamily G member 2; breast cancer resistance protein/mitoxantrone resistance protein) and although it has been reported that this drug has the ability to reverse ABCB1 (ABC subfamily B member 1; P-glycoprotein)- and ABCG2-mediated multidrug resistance in cancer cells [9–11], the mechanism by which gefitinib is taken up into the cell is still unknown.

In addition to the transporters involved in drug efflux a number of transporters are responsible for drug uptake. The major influx proteins belong to the largest superfamily of transporters, the solute carrier (SLC) superfamily [12,13]. This group of transporters includes the SLC22 family encompassing the organic cation transporters (hOCTs), the novel organic cation transporters (OCTNs) and the organic anion transporters (OATs). The hOCTs possess an affinity for positively charged endogenous (epinephrine, norephinephrine, etc.) and exogenous substances (1-methyl-4-phenylpyridinium (MPP), tetraethylammonium (TEA), quinine) [12]. In addition, several drugs have been identified as hOCTs substrates and their number is increasing. hOCTs substrates include antiviral drugs, the anti-diabetic drug metformin [14], anticancer drugs cisplatin and oxaliplatin [15,16], doxorubicin [17] and the tyrosine kinase inhibitor imatinib [18,19]. In view of our previous experience on nutrient transport [20–22], we characterized the influx of gefitinib and analyzed the functional characteristics of the transporter in a panel of NSCLC cell lines. Noteworthy aspects of this study are the possible pharmacological interaction between gefitinib and other drugs during cellular uptake and the determination of the intracellular concentration of gefitinib required to inhibit EGFR autophosphorylation in cells carrying wild-type or mutant receptors.

2. Materials and methods

2.1. Cell culture

The human NSCLC cell lines H322, H1299, Calu-1, H1975, PC9 and SKLU-1 were cultured as recommended. All media were supplemented with 2 mM glutamine, 10% fetal bovine serum (FBS Gibco, Life Technologies). Cell lines were from the American Type Culture Collection (Manassas, VA, USA) and were maintained under standard cell culture conditions at 37 °C in a water-saturated atmosphere of 5% CO_2 in air.

The H1975 cell line was kindly provided by Dr. E. Giovannetti (Department of Medical Oncology, VU University Medical Center, Amsterdam, The Netherlands), and the PC9 cell line was kindly provided by Dr P. Janne (Dana-Farber Cancer Institute, Boston, MA). A table listing the characteristics of the cell lines has been recently published by our group [4] and as reported, cells showing IC_{50} for gefitinib <1 μM were considered sensitive (PC9, H322) and cell lines with $IC_{50} > 8$ μM (SKLU-1, Calu-1, H1975, H1299) were considered resistant.

HEK293 cells stably transfected with hOCT1 and hOCT2 were kindly provided by Dr. H. Koepsell (Institute of Anatomy and Cell Biology, Würzburg, Germany) and were cultured in Dulbecco's modified Eagle's medium supplemented with G418 sulfate (600 μg/mL, Sigma–Aldrich, St. Louis, MO, USA).

2.2. Drug treatment

Gefitinib (ZD1839/Iressa) was synthesized as described elsewhere [23]. In all assays, the drug was dissolved in DMSO immediately before its addition to the media. The concentration of DMSO never exceeded 0.1% (v/v) and equal amounts of the solvent were added to control cells. The prototypical cations MPP, TEA and the inhibitors prazosin, procainamide, quinidine, verapamil, corticosterone, carnitine, choline, β-estradiol were purchased from Sigma–Aldrich (St. Louis, MO, USA).

2.3. Transport measurements

Labeled [^{3}H]gefitinib (7.64 Ci/mmol) and labeled N-[Methyl-^{3}H]MPP(+) (86.4 Ci/mmol) were respectively custom made by and purchased from Perkin Elmer (Boston, MA, USA). In all the experiments radiolabeled drug was mixed with unlabeled drug to reach the desired final concentration. The measurements of [^{3}H]gefitinib and N-[Metil-^{3}H] MPP uptake by cells were essentially performed as described previously for amino acids [20] and creatine [21] with minor modifications. Cells were seeded into 4 cm^2 wells of disposable multiwell trays (NUNC, Rosekilde, Danmark) to give the desired cell density, and incubated for 48 h in complete growth medium at 37 °C. After removing medium, the cells were quickly washed with Earle's balanced salt solution containing 0.1% glucose (uptake buffer) and immediately incubated in uptake buffer at 37 or 4 °C for the desired period of time in the presence of labeled gefitinib or MPP. For the cis-inhibition study, the uptake of [^{3}H]gefitinib or N-[Metil-^{3}H]-MPP was achieved by adding various concentrations of unlabeled inhibitors to the uptake buffer. For the trans-inhibition study the uptake of [^{3}H]gefitinib or N-[Metil-^{3}H]-MPP was measured after 15 min of preloading with unlabeled compounds. In some experiments the cells were incubated for 15 min at 37 °C in Earle solution prior to measurement of transport activity in order to reduce the intracellular levels of osmolytes, mainly amino acids (depletion phase). The Na^+-free buffer was modified by replacing NaCl with equimolar concentration of choline chloride or lithium chloride. Uptake buffers of varying pH (5.5, 6.5, 7.5, 8.5) were prepared by adding 25 mM MES (pH 5.5), PIPES (pH 6.5), Hepes (pH 7.5) or Tris–HCl (pH 8.5) to uptake buffer without bicarbonate. For membrane potential alteration, K^+ was raised to intracellular concentration with the concomitant reduction in Na^+. The osmolalities of the different uptake buffers were checked with a vapour-pressure osmometer (Wescor) and values were close to 0.3 osmol (kg H_2O)$^{-1}$. The incubations were stopped by removal of the uptake buffer and the cells were quickly washed three times with fresh cold solution. Trichloroacetic acid (TCA, 5%, w/v) was added to denature the cells and the radioactivity in samples of the acid extracts was measured by scintillation counting. Cell proteins, precipitated by TCA, were dissolved in 0.5 N NaOH and their concentration determined by a dye-fixation method (Bio-Rad) using bovine serum albumin as standard [24].

2.4. EGFR autophosphorylation assay

Inhibition of EGFR autophosphorylation was determined using a specific anti-phosphotyrosine antibody by Western blot analysis (Cell Signaling Technology, Beverly, MA, USA) as previously described [25] and by specific enzyme-linked immunosorbent assays (ELISA) (Millipore S.A.S., Molsheim, F). Briefly, cells were preincubated for 10 min with the indicated concentrations of gefitinib before stimulation with 0.1 μg/ml EGF for 5 min. After protein extraction EGFR phosphorylation at the tyrosine residue at position 1068 was evaluated by Western blotting and by ELISA and normalized to protein content and to the total EGFR.

2.5. Determination of cell volume

Intracellular volumes were estimated by measurement of the equilibrium distribution of 3-O-methyl-D-[1-^{3}H]glucose as previously described [20] using the method of Kletzien et al. [26].

2.6. Real-Time RT-PCR

Total RNA was isolated by the TRIzol® reagent (Invitrogen, Carlsbad, CA, USA) and reverse-transcribed as previously described [21].

The transcript level of *SLC22A1*, *SLC22A2* and *SLC22A3* genes was assessed by Real-Time qRT-PCR on an iCycler iQ Multicolor RealTime PCR Detection System (Bio-Rad, Hercules, CA, USA).

The ProbeFinder software (Roche Diagnostics, Mannheim, Germany) was used to design specific primers, spanning the exon–exon junctions, and locked nucleic acid probes for target and control genes [*phosphoglycerate kinase 1* (*PGK1*), *ribosomal protein L13* (*RPL13*) and *hypoxanthine-guanine-phosphoribosyltransferase* (*HPRT*)]. Primers and probes included: SLC22A1-F (5′-TCCTCTTCCTGCTCTACTACTGG-3′), SLC22A1-R (5′-TGGTCCATTATCTTTATTGCTTCA-3′), SLC22A1-probe (5′FAM GGTGGCTG 3′DQ); SLC22A2-F (5′-TTCTTCTTCTTGCTCTATTACTGGTG-3′), SLC22A2-R (5′-GGCTTCAGCATTCTTATTCTGG-3′), SLC22A2-probe (5′FAM GGTGGCTG 3′DQ); SLC22A3-F (5′-AAGGAATCCAGTTAGCCATCAC-3′), SLC22A3-R (5′-TCCGAGTAATCAGCCAACG-3′), SLC22A3-probe, (5′-FAM GGAGGAAG 3′DQ); PGK1-F (5′-GGAGAACCTCCGCTTTCAT-3′), PGK1-R (5′-CTGGCTCGGCTTTAACCTT-3′), PGK1-probe (5′-FAM GGAGGAAG 3′DQ); RPL13-F (5′-ACAGCTGCTCAGCTTCACCT-3′), RPL13-R (5′-TGGCAGCATGCCATAAATAG-3′), RPL13-probe (5′-FAM CAGTGGCA 3′DQ); HPRT-F (5′-TGACCTTGATTTATTTTGCATACC-3′), HPRT-R (5′CGAGCAAGCGAGCAAGACGTTCAGTCCT-3′), HPRT-probe (5′-FAM GCTGAGGA 3′DQ).

Duplicate assays were run for each sample and each plate included a standard curve and both a negative (water instead of cDNA) and a positive (cDNA from HEK293 cells) control. The relative transcript quantification was calculated by the *geNorm* algorithm for Microsoft Excel™ after normalization by expression of the control genes and expressed in terms of arbitrary units (a.u.).

2.7. Determination of lactate production

Medium and intracellular lactate concentration was determined spectrophotometrically by an enzymatic assay (Biovision) according to the instructions of the manufacturer and absorbance

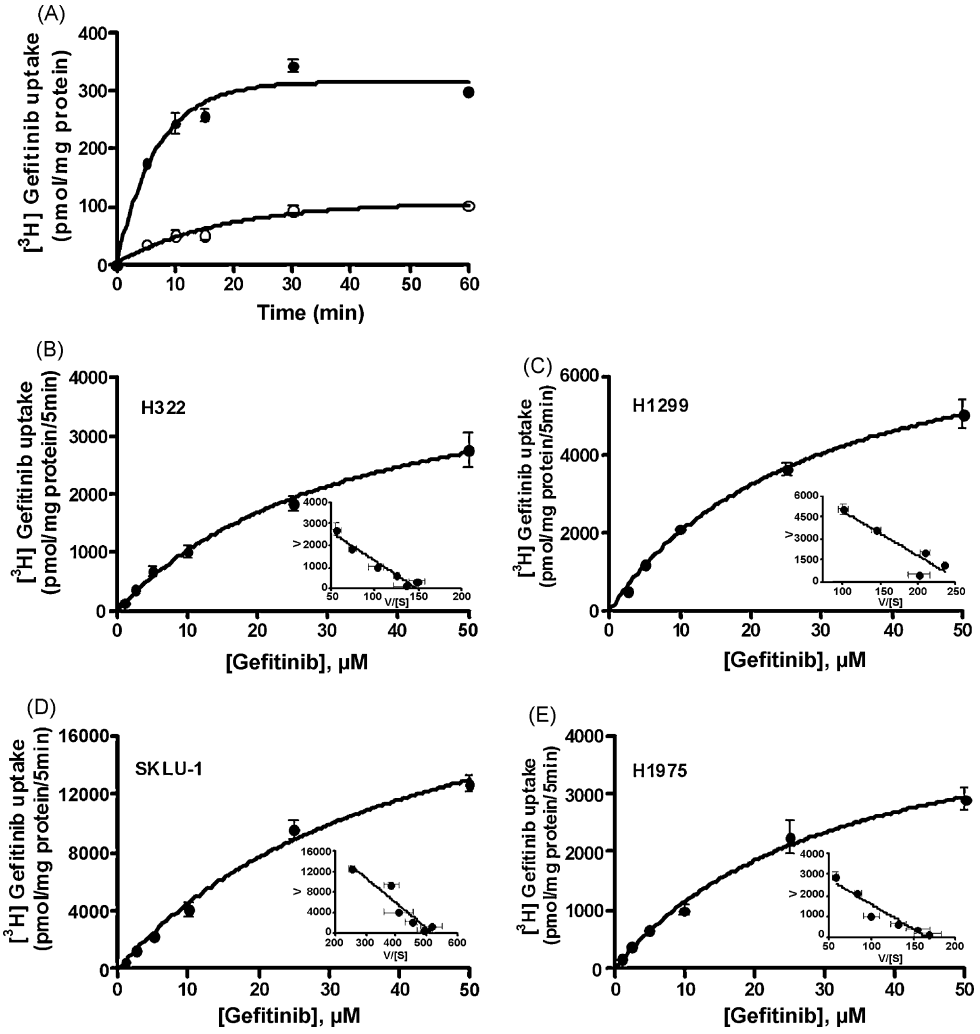

Fig. 1. Time course and kinetic characteristics of [^{3}H]gefitinib uptake in NSCLC cell lines. (A) Time course of 1 µM [^{3}H]gefitinib uptake at 37 °C (●) and 4 °C (○) in H322 cell line. Each point represents the mean ± SD of four independent determinations. The time course was fitted to the experimental data by a non-linear regression analysis. The kinetic characteristics of [^{3}H]gefitinib uptake were evaluated in H322 (B), H1299 (C), SKLU-1 (D) and H1975 (E). Cells were incubated for 5 min with [^{3}H]gefitinib at concentrations ranging from 1 to 50 µM. Specific uptake was calculated by subtracting the values at 4 °C from those at 37 °C. Each point represents the mean ± SD of four independent determinations. Data were analyzed by the Eadie-Hofstee method (inset); linear regression analysis was used to calculate the parameters of the curves (R^2 values were >0.99).

read at 570 nm. Intracellular lactate was extracted with ice 10% acetic acid and the acid-soluble supernatant was lyophilized and assayed upon resuspension in PBS.

The results were expressed as nmol (intracellular) or μmol (extracellular) of lactate, per milligram of protein.

2.8. Kinetic and statistical analysis

The kinetic and statistical analyses were carried out using GraphPad Prism version 5.00 software (GraphPad Software Inc., San Diego, CA). Results are expressed as mean values ± standard deviations (SD) for the indicated number of independent measurements. The K_m and V_{max} values were obtained by fitting the Michaelis-Menten equation to the data. IC_{50} values for inhibition of gefitinib uptake by cationic transporter inhibitors were calculated by fitting the experimental data with a hyperbolic function and constraining Y_{max} to 100.

The significance of differences between the mean values recorded for different experimental conditions was calculated by the Student's *t*-test, and *P* values are indicated where appropriate in the figures and in their legends. A *P*-value <0.05 was considered as significant.

3. Results

3.1. Time course and kinetics of gefitinib uptake

We first examined the time-course of [^{3}H]gefitinib uptake at a concentration of 1 μM at 37 °C or 4 °C in H322 cells (Fig. 1A). We observed a significant difference in the uptake at 4 °C compared with 37 °C at all time points suggesting that gefitinib uptake is an active process. The passive influx component at 4 °C never exceeded 20% of the total influx. The uptake at 37 °C increased in a time-dependent manner and it was almost linear with time up to 10 min reaching a plateau at 15 min. The kinetics of the active transport were then evaluated in H322 (gefitinib-sensitive cell line), H1299, SKLU-1 and H1975 cells (resistant-cell lines) [4] (Fig. 1B–E). Cells were incubated for 5 min with [^{3}H]gefitinib at concentrations ranging between 1 and 50 μM and non-mediated passive influx was subtracted before performing kinetic analysis. The mediated uptake as computed by non-linear regression analysis yielded similar Michaelis–Menten constants (K_m values, μM) among the cell lines tested (34 ± 5 in H322, 29.84 ± 2.9 in H1299, 32.5 ± 6.4 in H1975, 43 ± 9.4 in SKLU-1) and different V_{max} values (pmol/mg of protein/5 min) (4564 ± 352 in H322, 8010 ± 397 in H1299, 4873 ± 494 in H1975 and 24174 ± 3006 in SKLU-1).

The Eady–Hofstee plot (inset) showed a single straight line suggesting that specific gefitinib uptake was mediated by a single component in these NSCLC cell lines.

3.2. Effects of extracellular Na^+ removal, membrane depolarization, pH and cell density on [^{3}H]gefitinib uptake

To further explore the characteristics of the gefitinib transport system, we analyzed in H322 cells the Na^+-, potential- and pH-dependence of [^{3}H]gefitinib uptake.

When Na^+ was replaced with choline chloride or lithium chloride (Fig. 2A) no significant difference was detected suggesting that the uptake of gefitinib was independent of extracellular Na^+ and of high level of choline. Moreover, despite a large increase in extracellular K^+ concentration (110 mM) gefitinib uptake was unaffected indicating that depolarization of the membrane potential did not modify the transport activity. Our experimental results, not shown, indicated that the depletion of intracellular nutrients (mainly amino acids) did not affect the initial rate of [^{3}H]gefitinib uptake suggesting that mechanisms of trans-inhibition or trans-stimulation by physiological osmolytes were not involved in the regulation of this transport system.

As shown in Fig. 2B [^{3}H]gefitinib uptake was found to be significantly reduced by changing the extracellular pH from 7.5 to 6.5 and 5.5.

Since cell density can regulate the activity of transport systems in cultured cells [20] we measured the uptake of gefitinib in cells seeded at different densities at 4 and 37 °C. In Calu-1 (Fig. 2C) and in other cell lines (not shown) only the rate of mediated transport markedly decreased with increasing cell density suggesting that cell density might change the number of effective carrier molecules or their mobility within the cell membrane.

3.3. Effects of different inhibitors on gefitinib cellular uptake

We then analyzed the inhibitory effect of different cationic organic compounds on the gefitinib uptake in H322 cells (Fig. 3A) by using different cationic transporter substrates/inhibitors (panel B, Fig. 3) [12]. Prazosin, procainamide, verapamil and quinidine

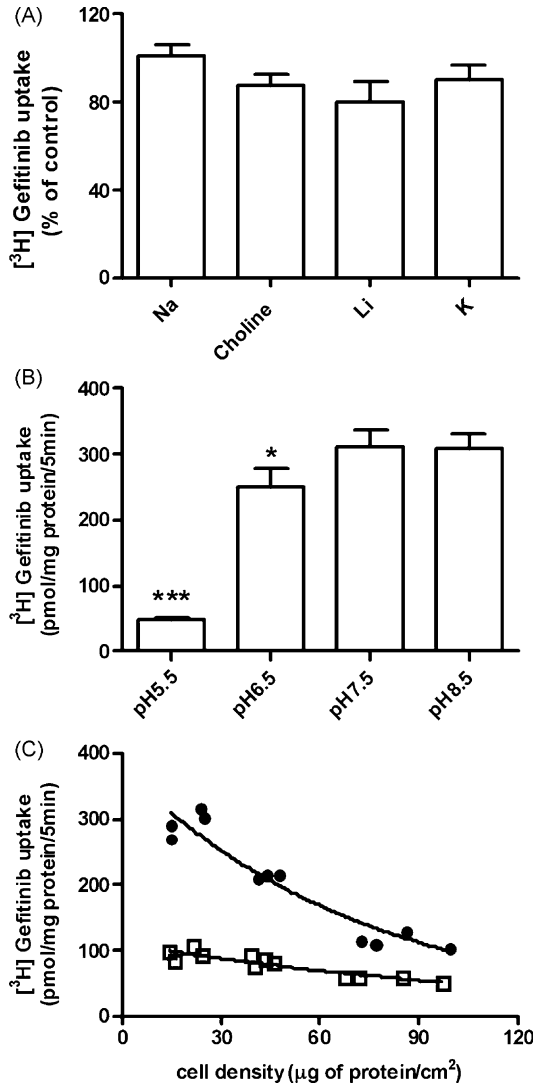

Fig. 2. Influence of Na^+, membrane potential, pH and cell density on [^{3}H]gefitinib uptake in H322 cell line. The initial rate (5 min) of 1 μM [^{3}H]gefitinib was measured in the presence of NaCl (control), choline chloride, LiCl and KCl as the main osmolyte (A); as function of different pH values during uptake (B) and of cell density (C) at 4 °C (□) and 37–4 °C (●). Values given are the means (±SD) of four independent determinations and the significance of differences between the mean values was calculated by Student's *t*-test ($^*P < 0.05$; $^{***}P < 0.001$).

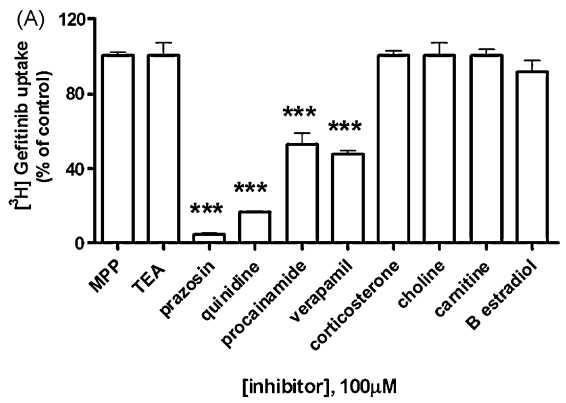

(B)

Substrate/inhibitors	hOCT1	hOCT2	hOCT3	hOCT6	hOCTN1	hOCTN2
MPP	++	++	++			+
TEA	++	++	+	++	+	+
PRAZOSIN	++		+			
QUINIDINE	++				+	+
PROCAINAMIDE	+	++				
VERAPAMIL	++					
CORTICOSTERONE	+		++			
CHOLINE		+			+	
CARNITINE				++	++	++
β ESTRADIOL			++			

++ high specifity; + low specifity

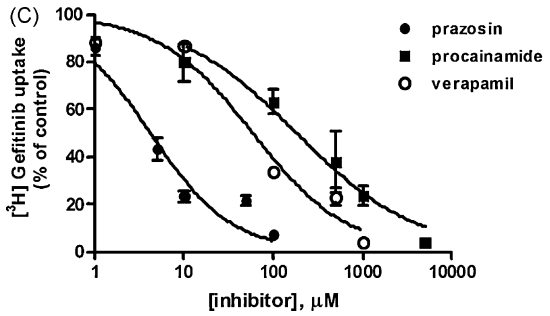

Fig. 3. Inhibition of [^{3}H]gefitinib uptake by different agents. (A) H322 cells were incubated with 0.1 μM [^{3}H]gefitinib for 5 min in the absence or presence of 100 μM cationic-substrate/inhibitors referring to the results cited from the review article by Koepsell et al. [12] as indicated in the panel (B). Prazosin, quinidine, procainamide and verapamil significantly inhibited gefitinib uptake (***$P < 0.001$). (C) Concentration-dependent inhibition of [^{3}H]gefitinib uptake (1 μM) by prazosin, procainamide and verapamil. Values given are the means (±SD) of four independent determinations and are expressed in percent of control.

markedly decreased gefitinib uptake, while corticosterone, carnitine, choline, β-estradiol and the prototypical organic cations TEA and MPP did not significantly reduce gefitinib uptake. Moreover, TEA and MPP failed to inhibit gefitinib uptake up to 5 mM (data not shown). Similar results were obtained in Calu-1 cells (not shown).

The IC_{50} values for prazosin, procainamide and verapamil inhibition of [^{3}H]gefitinib uptake were calculated from the inhibition curves shown in Fig. 3C. Prazosin showed the highest potency (IC_{50} 4.2 ± 1.3 μM), while procainamide and verapamil were less effective (IC_{50} 182 ± 1.3 and 59 ± 1.4 μM, respectively).

Because of the positive results obtained with substrates/inhibitors, the expression of the mRNA for hOCT1, hOCT2 and hOCT-3 was then investigated by RT-PCR in H322, H1299, Calu-1, SKLU-1 and H1975 cell lines (Fig. 4A). hOCT2 was not detected while hOCT1 was expressed in all the cell lines, except for H1299, even though the expression levels showed substantial differences among these cell types; hOCT3 was expressed at higher levels in four of the five cell lines tested (H1299, Calu-1, SKLU-1, H1975).

In the light of the gefitinib-uptake results, we concluded that there was no correlation between gefitinib uptake and hOCT1, hOCT2 or hOCT-3 expression. In fact, gefitinib was actively transported in H1299 lacking hOCT1 expression and in H322 lacking hOCT-3 expression; moreover, all the cell lines were null for hOCT2 expression.

This conclusion was also supported by measuring MPP and gefitinib uptake in kidney embryonic HEK293 cells overexpressing hOCT1 and hOCT2. As shown in Fig. 4B and C hOCT1 and hOCT2 overexpression significantly increased the uptake of N-[Metil-^{3}H] MPP but did not affect the uptake of [^{3}H]gefitinib. However, cis-inhibition experiments demonstrated that gefitinib significantly reduced N-[Metil-^{3}H] MPP uptake in overexpressing hOCT1 and to lesser extent in overexpressing hOCT2 HEK293 cells (Fig. 4D) suggesting that gefitinib affected hOCT1 and hOCT2 transport function but not as a competitive substrate. This conclusion is also supported by trans-inhibition experiments showing that uptake of MPP was significantly reduced when hOCT1 HEK293 cells were preloaded with gefitinib (not shown).

3.4. Effect of the intracellular concentration of gefitinib on the inhibition of EGFR autophosphorylation

We then analyzed the effect of different intracellular concentrations of gefitinib, obtained by varying the extracellular concentration, on the level of EGFR autophosphorylation in NSCLC cell lines characterized by different EGFR status (wild type *vs* mutant). The intracellular concentration of gefitinib was obtained by dividing the gefitinib content, expressed as pmol/mg of protein/15 min, by the corresponding values of cell volume recorded under the same experimental conditions.

As reported in Fig. 5A gefitinib was concentrated in the intracellular compartment in all cell lines, with a ratio in/out between one hundred and three hundred depending on the extracellular level and the cell line tested. It is of note that at 1 μM (the maximum plasma concentration of gefitinib observed at the clinically relevant dose (250 mg/day) [27]) the intracellular concentration in resistant-cell lines was similar (Calu-1) or even higher (H1299, SKLU-1, H1975) than that in gefitinib-sensitive (PC9 and H322) cells.

As shown in Fig. 5B in all the cell lines tested, EGF stimulation induced a significant phosphorylation of tyr1068 and gefitinib inhibited EGFR autophosphorylation in a dose-dependent manner. We demonstrated a significant correlation between the intracellular gefitinib concentration and the inhibition of EGFR phosphorylation in all cell lines except H1975 (carrying T790 M mutation). Intracellular concentrations of gefitinib that completely inhibit EGFR autophosphorylation ranged from 150 to 300 μM in cell

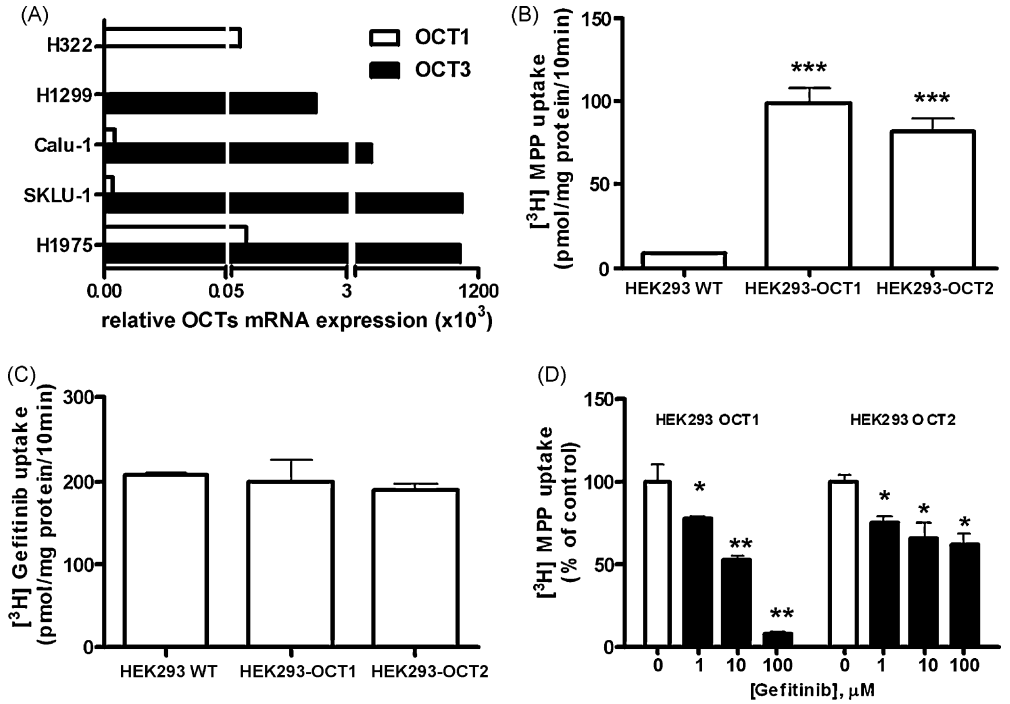

Fig. 4. Effect of hOCTs expression on [^{3}H]gefitinib transport. (A) The expression of hOCT1, hOCT-2 and hOCT-3 in NSCLC cell lines was detected by RT-PCR as described in Section 2. The experimental conditions used for RT-PCR were validated using as positive control mRNA isolated from stably transfected HEK293 cells. The cellular uptake at 1 μM of the substrates [^{3}H] MPP (B) or [^{3}H]gefitinib (C) was determined in hOCT1- and hOCT2-HEK293 transfected cells and in the corresponding MOCK cells (WT). Values given are the means (±SD) of three independent determinations (***$P < 0.001$ versus mock cells). (D) Stably transfected HEK293-hOCT1 and HEK293-hOCT2 cells were incubated with 3 nM [^{3}H] MPP for 5 min. The uptake of [^{3}H]MPP was determined both in the absence (empty columns) or in the presence (filled columns) of increasing concentration of gefitinib (1–100 μM). Values given are the means (±SD) of three independent determinations and are expressed in percent of control. *$P < 0.05$; **$P < 0.01$; versus control.

models carrying wild-type receptor (H322, H1299, Calu-1, SKLU-1). The PC9 cell line, harbouring a deletion mutation on exon 19 of the EGFR gene (delE746-A750), showed maximal inhibition at intracellular gefitinib concentration of 10 μM whereas H1975 showed no inhibition up to 1 mM.

3.5. Effect of cell density and lactate on intracellular gefitinib accumulation and EGFR autophosphorylation

Since cell density and extracellular pH affected gefitinib uptake (see Fig. 2B and C), we investigated the effect of high density and

(A)

[Extra cellular gefitinib], μM	[Intra cellular gefitinib], μM					
	PC9	*H322*	*H1299*	*Calu-1*	*Sklu-1*	*H1975*
0.003	0.34 ± 0.001	0.51 ± 0.007	0.68 ± 0.02	0.50 ± 0.02	0.79 ± 0.05	0.44 ± 0.02
0.01	1.11 ± 0.05	1.50 ± 0.13	2.07 ± 0.18	1.71 ± 0.15	2.58 ± 0.12	1.78 ± 0.21
0.1	11 ± 0.719	17 ± 0.64	23 ± 1.57	17 ± 1.38	31 ± 0.58	19 ± 1.34
1	127 ± 7.47	128 ± 7.07	189 *** ± 6.53	123 ± 1.24	329 *** ± 10.07	206 *** ± 1.49

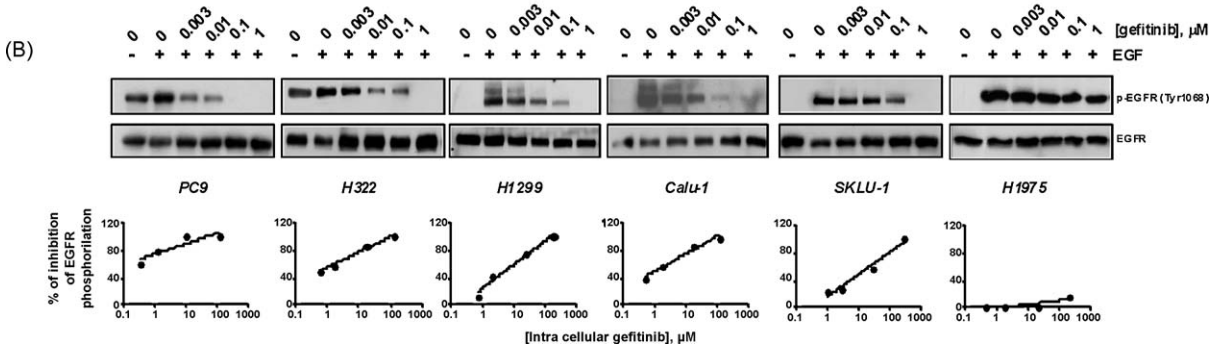

Fig. 5. Intracellular gefitinib concentration in NSCLC cell lines and its effect on EGFR autophosphorylation. (A) NSCLC cell lines were incubated with the indicated extracellular [^{3}H]gefitinib concentration for 15 min and then intracellular gefitinib concentration was calculated by dividing the gefitinib content expressed as pmol/mg of protein by the corresponding values of cell volume recorded in the same experimental condition as described in Section 2. (B) NSCLC cells were incubated for 10 min with the indicated extracellular concentrations of gefitinib before stimulation with 0.1 μg/ml EGF for 5 min. Western blot analysis was performed by using monoclonal antibodies directed to p-EGFR(p-Tyr1068) and to EGFR.
The experiment, repeated three times, yielded similar results. The immunoreactive spots at each point were quantified by densitometric analysis, ratios of phosphotyrosine/total EGFR were calculated, values were expressed as percentage of inhibition versus control and were plotted as function of the intracellular concentration of gefitinib. Similar results were obtained by using ELISA kit to calculate the percentage of inhibition versus control.

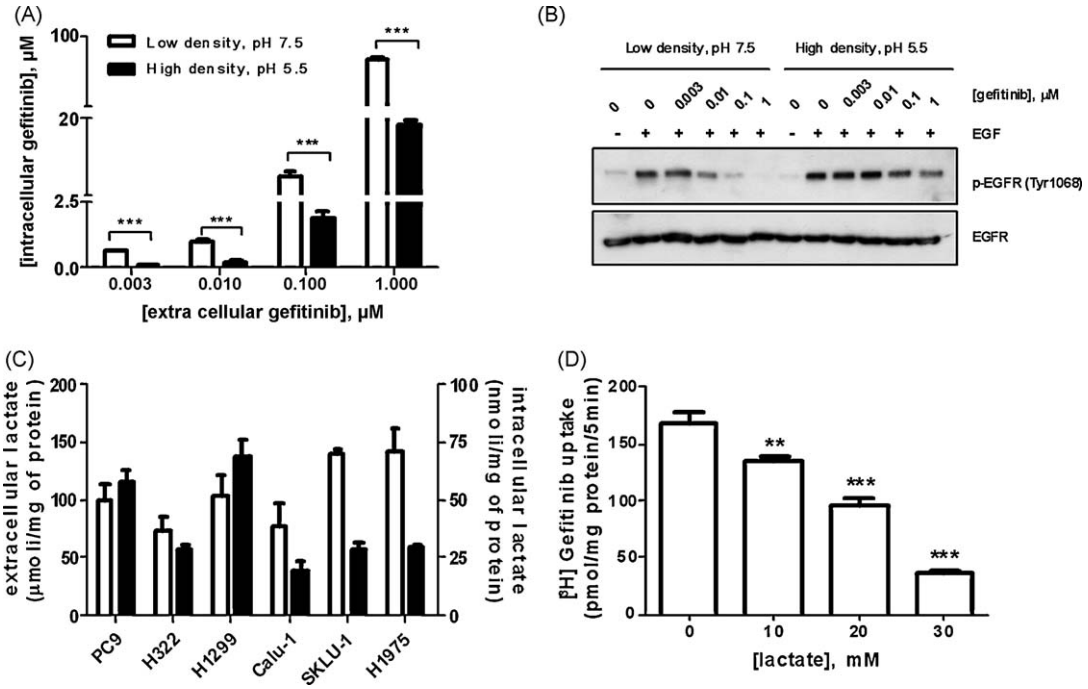

Fig. 6. Effect of cell density, lactate production and extracellular pH on intracellular gefitinib concentration and EGFR autophosphorylation. (A) H322 cells were seeded al low (7000 cells/cm^2) and high (70 000 cells/cm^2) density and after 48 h incubated for 15 min with the indicated extracellular [^{3}H]gefitinib concentration in uptake buffer at pH 7.5 for low density and pH 5.5 for high density respectively. The intracellular gefitinib concentration was determined as described in the legend of Fig. 5A (***$P < 0.001$). (B) H322 cells were seeded al low (7000 cells/cm^2) and high (70 000 cells/cm^2) density and after 24 h were incubated for 10 min with the indicated extracellular concentrations of gefitinib before stimulation with 0.1 µg/ml EGF for 5 min in the presence of buffer at pH 7.5 for low density and pH 5.5 for high density respectively. Western blot analysis was performed by using monoclonal antibodies directed to p-EGFR(p-Tyr1068) and to EGFR. The experiment, repeated three times, yielded similar results. (C) NSCLC cell lines were seeded at high density and after 48 h of incubation the intracellular and extracellular lactate levels were determined as described in Section 2. Lactate level calculated for each cell line were normalized to protein content and expressed as nmol (intracellular, filled columns) or µmol (extracellular, empty columns) of lactate, per milligram of protein. Values given are the means (±SD) of three independent determinations. D) The initial rate (5 min) of 1 µM [^{3}H]gefitinib was measured in the presence of increased concentration of lactate in H322 cell line. Values given are the means (±SD) of three independent determinations (**$P < 0.01$; ***$P < 0.001$; versus control).

low pH on intracellular gefitinib content and inhibition of EGFR autophosphorylation in the H322 cell line. As shown in Fig. 6A, cells at high density exposed to pH 5.5 accumulated levels of gefitinib more than five times lower than cells at low density exposed to physiological pH; consequently the EGFR autophosphorylation, evaluated by Western blotting and shown in Fig. 6B, was only partially reduced at 1 µM gefitinib.

In most of our cell lines phenol red, present in culture media, exhibited a gradual color transition from red to yellow over the pH range 7.5–6, more evident in cell cultured at high density. Since this acidification of extracellular compartment could be associated with production of lactate we measured the level of lactate in the intracellular compartment and in the medium in some sensitive and resistant cells after 48 h of incubation.

As shown in Fig. 6C a significant production of lactate was observed in all the cell lines tested irrespective of sensitivity to gefitinib and lactate production acidified the extracellular compartment in a dose dependent manner. On the basis of extracellular concentration of lactate extruded by the cells (ranging between 10 and 30 mM) we tested the effect of different concentrations of lactate on gefitinib uptake in H322 cell line (Fig. 6D). 10 mM lactate (pH 6.6) inhibited gefitinib uptake by 20% and the inhibition was more than 80% at 30 mM (pH 5.0). These data suggest that the extrusion of lactate may contribute in decreasing the pH, which in turn can influence the uptake and the intracellular accumulation of gefinitib.

4. Discussion

Gefitinib is a reversible competitive inhibitor of the tyrosine kinase domain of EGFR, and has been shown to have antitumor activity in a subset of patients with NSCLC (10% of patients from Europe and 30% from East Asia) [2,3,28]. Tumors responding to EGFR TKIs harbour mutations in the tyrosine kinase domain, the most frequent being L858R and Del (746–750), and the mutant kinases showed a reduced affinity for ATP and increased affinity for gefitinib [29].

Gefitinib is dosed at 250 mg/day, it is absorbed by 60% after oral administration and once absorbed it is 90% plasma protein-bound [28]. Gefitinib is extensively distributed in tissues with the highest levels being found in liver, kidney, gastrointestinal tract and lung as evaluated by a rat tissue distribution study [30]. In tumor xenograft models, gefitinib tumor concentrations were much higher than the corresponding plasma concentration [31] and in a pilot Phase II study in early stage NSCLC, intratumor gefitinib levels of about 33 µM versus 0.5 µM in plasma after 28 days of gefitinib treatment were reported [32]. Our research was designed to supplement this information by studying the gefitinib uptake in different lung cancer cell lines and by exploring its possible relationship with gefitinib resistance and sensitivity. To our knowledge, no studies designed to identify the mechanisms involved in cellular uptake of gefitinib have been reported.

Recent studies showed that imatinib, a tyrosin kinase inhibitor effective in the treatment of chronic myeloid leukemia and gastrointestinal stromal tumor, is taken up by an active cellular process, mediated by hOCT1 in a variety of leukemia cell lines [18,33] and by hOCTN2 in transfected HEK293 cells [34]. On the other hand, no evidence for active uptake has been found for the second generation of BCR-ABL tyrosine kinase inhibitors dasatinib and nilotinib [35,36], nor for the multikinase inhibitors sorafenib and sunitinib [37].

Our results demonstrated that uptake of gefitinib was predominantly an active rather than a passive process as demonstrated by the temperature dependency of the uptake process and the concentrative activity of the transporter which was able to concentrate gefitinib intracellularly more than two hundred times depending on the extracellular concentration and the cell model analyzed. Analysis of the relation between initial velocity of gefitinib transport and substrate concentration suggested that only a high-affinity saturable transport component contributes to total gefitinib uptake. The affinity (K_m) of the carriers for substrate was similar in all the cell models tested, while the capacity (V_{max}) of the system of mediation and the intracellular concentration of gefitinib, as shown in Fig. 5A, was significantly higher in H1299 and SKLU-1 cells. This result is consistent with the interpretation that these cells have an increased number of transporters or a higher rate of transfer of the gefitinib-carrier complex across the membrane.

The gefitinib uptake was sodium- and potential-independent, but was sensitive to changes in cell density and extracellular pH, with inhibition of the transport activity at high density and low extracellular pH. Changing the extracellular pH can either affect the protonation state and consequently the charge of the substrate and/or the substrate binding pocket of the transporter under investigation. Moreover, in our study we demonstrated that in cells maintained at low density and at pH 7.5, the intracellular accumulation of gefitinib was five times higher than in cells maintained at high density and low pH (see Fig. 6); in these cells the EGFR autophosphorylation was still evident in the presence of 1 μM gefitinib, a concentration that completely inhibited EGFR autophosphorylation in a panel of NSCLC cell lines harbouring wild-type receptor [4].

The production of lactic acid under aerobic or anaerobic conditions contributes to the acidic microenvironment in many types of tumor [38]. Lactate is extruded by proton-coupled monocarboxylate transporters MCTs [39], mainly to avoid cytotoxic intracellular accumulation.

We measured the level of lactate in the intracellular compartment and in the medium in sensitive and resistant cells and we found a significant production and accumulation of lactate both inside and outside the cells. Moreover, the lactate level correlated with a decrease in extracellular pH and significantly affected gefitinib uptake.

Our results suggest that the uptake of gefitinib and consequently the inhibition of the EGFR signaling might be reduced in tumors characterized by elevated lactate production.

Since at physiological pH gefitinib is an organic cation, in our search for gefitinib transporters we examined eleven compounds known to be selective inhibitors of hOCTs and of hOCTNs (see panel B, Fig. 3; [12]). Only the hOCT1 inhibitors tested (prazosin, quinidine, procainamide and verapamil) significantly inhibited the uptake of gefitinib; prazosin exhibiting the highest potency (IC_{50}: 4.2 μM). However, discrepancies were observed between the inhibition values for hOCTs prototypical substrates (MPP and TEA) obtained in this study and those reported in the literature, as these compounds did not inhibit gefitinib uptake up to 5 mM.

hOCT1 mRNA is well expressed in NSCLC cell lines as reported in previous studies on human tissues [40,41]. In accordance with the observation that gefitinib was actively transported in H1299 lacking hOCT1 expression, our data using a stably transfected cell line model indicate that hOCT1 was not involved in the uptake of gefitinib despite the inhibitory effect exerted by some hOCT1 inhibitors. RT-PCR data also showed that hOCT-3 mRNA was expressed in many of the cell line tested; however, corticosterone and β-estradiol (hOCT3 inhibitors) did not affect gefitinib uptake in Calu-1 cells and on the other hand H322, lacking hOCT-3 expression, significantly took up and accumulated gefitinib.

Choline has a similar chemical structure to gefitinib [42] and as an organic cation is known to be a substrate for hOCTs. hOCT-1 and hOCT-2 accept choline as a substrate with low affinity, hOCT-3 does not recognize choline as a substrate [43]. A different member of the choline transporter family unrelated to hOCT or CHT (high-affinity choline transporters) subgroup and named choline transporter-like protein 1 (CTL1) has been characterized in neuronal and tumor tissues including lung adenocarcinoma [43,44]. It has been reported that gefitinib reduced uptake of labeled choline, mainly mediated by CTL1, in A549 lung cancer cell line [42]. However, our cis-inhibition experiments showed that a high level of choline (see Fig. 2A) did not inhibit gefitinib uptake, suggesting that CTL-1 did not contribute to the transport of gefitinib.

During cancer therapy, gefitinib is often co-administered with a range of other drugs. It is of note that gefitinib significantly reduced uptake of MPP in hOCT1 and hOCT2 overexpressing cells, suggesting that gefitinib exerts an inhibitory effect on the intracellular accumulation of drugs transported by hOCT1 and hOCT2 such as metformin, an anti-diabetic drug [14]; oxaliplatin [16]; cisplatin [15]; quinine, an antimalarial drug and debrisoquine, an antihypertensive drug [12,45]. Therefore co-administration of these drugs with gefitinib may inhibit their uptake and may have a clinically relevant impact. For instance, the concomitant use of gefitinib with metformin may compromise optimal glycemic control in diabetic patients.

Gefitinib was highly concentrated in the intracellular compartment in all cell lines tested. However, at 1 μM, the average plasma concentration of gefitinib obtained at the clinically administered dose [27], the intracellular concentration in resistant-cell lines was higher than in gefitinib-sensitive cells and in any case largely sufficient to inhibit EGFR autophosphorylation.

On the basis of these results, one of the proposed mechanisms for the development of resistance to gefitinib [5] and other TKI [18,19,33], i.e. a reduced concentration of the bioactive drug within the cells, can be ruled out. However, at present, we cannot exclude that over longer periods of incubation, gefitinib might be metabolized and extruded differently by gefitinib-resistant and -sensitive cells.

Acknowledgements

This work was supported by AIRC (Associazione Italiana per la Ricerca sul Cancro); Associazione Davide Rodella, Montichiari, BS; Ministero della Salute (Programma straordinario di ricerca oncologica 2006) Regione Emilia Romagna; Associazione Marta Nurizzo, Brugherio MI; CONAD, Bologna; Associazione Chiara Tassoni, Parma; A.VO.PRO.RI.T., Parma and Lega Italiana per la lotta contro i tumori, Sezione di Parma.

We thank Dr. H. Koepsell for providing us with HEK293 cells transfected with organic ion transporters, Dr E. Giovannetti for providing us with H1975 cell line and Dr. P. Janne for providing us with PC9 cell line.

References

[1] Ciardiello F, Tortora G. EGFR antagonists in cancer treatment. N Engl J Med 2008;358:1160–74.
[2] Reck M. Gefitinib in the treatment of advanced non-small-cell lung cancer. Expert Rev Anticancer Ther 2009;9:401–12.
[3] Gazdar AF. Activating and resistance mutations of EGFR in non-small-cell lung cancer: role in clinical response to EGFR tyrosine kinase inhibitors. Oncogene 2009;28(Suppl. 1):S24–31.
[4] La Monica S, Galetti M, Alfieri RR, Cavazzoni A, Ardizzoni A, Tiseo M, et al. Everolimus restores gefitinib sensitivity in resistant non-small cell lung cancer cell lines. Biochem Pharmacol 2009;78:460–8.
[5] Sequist LV, Martins RG, Spigel D, Grunberg SM, Spira A, Janne PA, et al. First-line gefitinib in patients with advanced non-small-cell lung cancer harboring somatic EGFR mutations. J Clin Oncol 2008;26:2442–9.

[6] Morgillo F, Lee HY. Resistance to epidermal growth factor receptor-targeted therapy. Drug Resist Updat 2005;8:298–310.
[7] Engelman JA, Janne PA. Mechanisms of acquired resistance to epidermal growth factor receptor tyrosine kinase inhibitors in non-small cell lung cancer. Clin Cancer Res 2008;14:2895–9.
[8] Huang Y, Sadee W. Membrane transporters and channels in chemoresistance and -sensitivity of tumor cells. Cancer Lett 2006;239:168–82.
[9] Ozvegy-Laczka C, Cserepes J, Elkind NB, Sarkadi B. Tyrosine kinase inhibitor resistance in cancer: role of ABC multidrug transporters. Drug Resist Updat 2005;8:15–26.
[10] Nakamura Y, Oka M, Soda H, Shiozawa K, Yoshikawa M, Itoh A, et al. Gefitinib (''Iressa'', ZD1839), an epidermal growth factor receptor tyrosine kinase inhibitor, reverses breast cancer resistance protein/ABCG2-mediated drug resistance. Cancer Res 2005;65:1541–6.
[11] Noguchi K, Katayama K, Mitsuhashi J, Sugimoto Y. Functions of the breast cancer resistance protein (BCRP/ABCG2) in chemotherapy. Adv Drug Deliv Rev 2009;61:26–33.
[12] Koepsell H, Lips K, Volk C. Polyspecific organic cation transporters: structure, function, physiological roles, and biopharmaceutical implications. Pharm Res 2007;24:1227–51.
[13] Ciarimboli G. Organic cation transporters. Xenobiotica 2008;38:936–71.
[14] Kimura N, Masuda S, Tanihara Y, Ueo H, Okuda M, Katsura T, et al. Metformin is a superior substrate for renal organic cation transporter OCT2 rather than hepatic OCT1. Drug Metab Pharmacokinet 2005;20:379–86.
[15] Ciarimboli G, Ludwig T, Lang D, Pavenstadt H, Koepsell H, Piechota HJ, et al. Cisplatin nephrotoxicity is critically mediated via the human organic cation transporter 2. Am J Pathol 2005;167:1477–84.
[16] Zhang S, Lovejoy KS, Shima JE, Lagpacan LL, Shu Y, Lapuk A, et al. Organic cation transporters are determinants of oxaliplatin cytotoxicity. Cancer Res 2006;66:8847–57.
[17] Okabe M, Unno M, Harigae H, Kaku M, Okitsu Y, Sasaki T, et al. Characterization of the organic cation transporter SLC22A16: a doxorubicin importer. Biochem Biophys Res Commun 2005;333:754–62.
[18] Thomas J, Wang L, Clark RE, Pirmohamed M. Active transport of imatinib into and out of cells: implications for drug resistance. Blood 2004;104:3739–45.
[19] Wang L, Giannoudis A, Lane S, Williamson P, Pirmohamed M, Clark RE. Expression of the uptake drug transporter hOCT1 is an important clinical determinant of the response to imatinib in chronic myeloid leukemia. Clin Pharmacol Ther 2008;83:258–64.
[20] Petronini PG, Alfieri RR, Losio MN, Caccamo AE, Cavazzoni A, Bonelli MA, et al. Induction of BGT-1 and amino acid system A transport activities in endothelial cells exposed to hyperosmolarity. Am J Physiol Regul Integr Comp Physiol 2000;279:R1580–9.
[21] Alfieri RR, Bonelli MA, Cavazzoni A, Brigotti M, Fumarola C, Sestili P, et al. Creatine as a compatible osmolyte in muscle cells exposed to hypertonic stress. J Physiol 2006;576:391–401.
[22] Alfieri RR, Petronini PG. Hyperosmotic stress response: comparison with other cellular stresses. Pflugers Arch 2007;454:173–85.
[23] Carmi C, Cavazzoni A, Zuliani V, Lodola A, Bordi F, Plazzi PV, et al. 5-benzylidene-hydantoins as new EGFR inhibitors with antiproliferative activity. Bioorg Med Chem Lett 2006;16:4021–5.
[24] Bradford MM. A rapid and sensitive method for the quantitation of microgram quantities of protein utilizing the principle of protein-dye binding. Anal Biochem 1976;72:248–54.
[25] Cavazzoni A, Galetti M, Fumarola C, Alfieri RR, Roz L, Andriani F, et al. Effect of inducible FHIT and p53 expression in the Calu-1 lung cancer cell line. Cancer Lett 2007;246:69–81.
[26] Kletzien RF, Pariza MW, Becker JE, Potter VR. A method using 3-O-methyl-D-glucose and phloretin for the determination of intracellular water space of cells in monolayer culture. Anal Biochem 1975;68:537–44.
[27] Sharma SV, Bell DW, Settleman J, Haber DA. Epidermal growth factor receptor mutations in lung cancer. Nat Rev Cancer 2007;7:169–81.
[28] Jiang H. Overview of gefitinib in non-small cell lung cancer: an Asian perspective. Jpn J Clin Oncol 2009;39:137–50.
[29] Carey KD, Garton AJ, Romero MS, Kahler J, Thomson S, Ross S, et al. Kinetic analysis of epidermal growth factor receptor somatic mutant proteins shows increased sensitivity to the epidermal growth factor receptor tyrosine kinase inhibitor, erlotinib. Cancer Res 2006;66:8163–71.
[30] McKillop D, Hutchison M, Partridge EA, Bushby N, Cooper CM, Clarkson-Jones JA, et al. Metabolic disposition of gefitinib, an epidermal growth factor receptor tyrosine kinase inhibitor, in rat, dog and man. Xenobiotica 2004;34:917–34.
[31] McKillop D, Partridge EA, Kemp JV, Spence MP, Kendrew J, Barnett S, et al. Tumor penetration of gefitinib (Iressa), an epidermal growth factor receptor tyrosine kinase inhibitor. Mol Cancer Ther 2005;4:641–9.
[32] Haura ESE, Becker D, McKillop D, Bepler G. Pilot phase II study of preoperative gefitinib in early stage non-small cell lung cancer with assessment of intratumor gefitinib levels and tumor target modulation. J Clin Oncol 2007;25 [abstract 7603].
[33] White DL, Saunders VA, Dang P, Engler J, Zannettino AC, Cambareri AC, et al. OCT-1-mediated influx is a key determinant of the intracellular uptake of imatinib but not nilotinib (AMN107): reduced OCT-1 activity is the cause of low in vitro sensitivity to imatinib. Blood 2006;108:697–704.
[34] Hu S, Franke RM, Filipski KK, Hu C, Orwick SJ, de Bruijn EA, et al. Interaction of imatinib with human organic ion carriers. Clin Cancer Res 2008;14:3141–8.
[35] Giannoudis A, Davies A, Lucas CM, Harris RJ, Pirmohamed M, Clark RE. Effective dasatinib uptake may occur without human organic cation transporter 1 (hOCT1): implications for the treatment of imatinib-resistant chronic myeloid leukemia. Blood 2008;112:3348–54.
[36] Davies A, Jordanides NE, Giannoudis A, Lucas CM, Hatziieremia S, Harris RJ, et al. Nilotinib concentration in cell lines and primary CD34(+) chronic myeloid leukemia cells is not mediated by active uptake or efflux by major drug transporters. Leukemia 2009;23:1999–2006.
[37] Hu S, Chen Z, Franke R, Orwick S, Zhao M, Rudek MA, et al. Interaction of the multikinase inhibitors sorafenib and sunitinib with solute carriers and ATP-binding cassette transporters. Clin Cancer Res 2009;15:6062–9.
[38] Tannock IF, Rotin D. Acid pH in tumors and its potential for therapeutic exploitation. Cancer Res 1989;49:4373–84.
[39] Halestrap AP, Meredith D. The SLC16 gene family-from monocarboxylate transporters (MCTs) to aromatic amino acid transporters and beyond. Pflugers Arch 2004;447:619–28.
[40] Nies AT, Koepsell H, Winter S, Burk O, Klein K, Kerb R, et al. Expression of organic cation transporters OCT1 (SLC22A1) and OCT3 (SLC22A3) is affected by genetic factors and cholestasis in human liver. Hepatology 2009;50:1227–40.
[41] Lips KS, Volk C, Schmitt BM, Pfeil U, Arndt P, Miska D, et al. Polyspecific cation transporters mediate luminal release of acetylcholine from bronchial epithelium. Am J Respir Cell Mol Biol 2005;33:79–88.
[42] Ishiguro N, Oyabu M, Sato T, Maeda T, Minami H, Tamai I. Decreased biosynthesis of lung surfactant constituent phosphatidylcholine due to inhibition of choline transporter by gefitinib in lung alveolar cells. Pharm Res 2008;25:417–27.
[43] Michel V, Yuan Z, Ramsubir S, Bakovic M. Choline transport for phospholipid synthesis. Exp Biol Med (Maywood) 2006;231:490–504.
[44] Wang T, Li J, Chen F, Zhao Y, He X, Wan D, et al. Choline transporters in human lung adenocarcinoma: expression and functional implications. Acta Biochim Biophys Sin (Shanghai) 2007;39:668–74.
[45] Hagenbuch B. Drug uptake systems in liver and kidney: a historic perspective. Clin Pharmacol Ther 2010;87:39–47.